IEEE Photonics Journal
An IEEE Photonics Society Publication

Open Access

The Orbital Angular Momentum Encoding System With Radial Indices of Laguerre–Gaussian Beam

Volume 10, Number 5, September 2018

Zhongyi Guo
Zikun Wang
Maxime Irene Dedo
Kai Guo

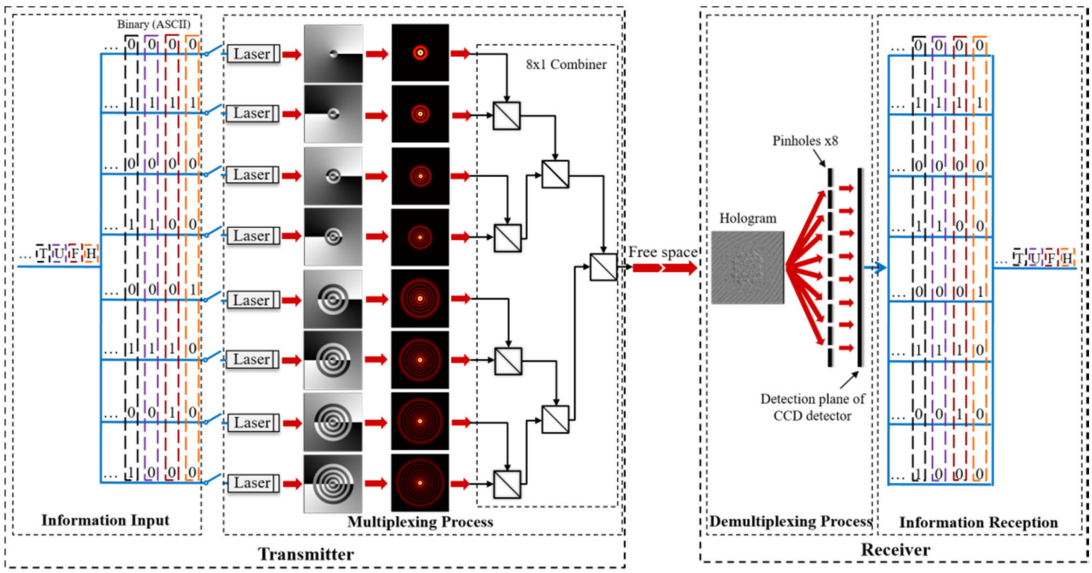

DOI: 10.1109/JPHOT.2018.2859807
1943-0655 © 2018 IEEE

The Orbital Angular Momentum Encoding System With Radial Indices of Laguerre–Gaussian Beam

Zhongyi Guo, Zikun Wang, Maxime Irene Dedo, and Kai Guo

School of Computer Science and Information Engineering, Hefei University of Technology, Hefei 230009, China

DOI:10.1109/JPHOT.2018.2859807

Manuscript received July 1, 2018; revised July 11, 2018; accepted July 14, 2018. Date of publication July 25, 2018; date of current version August 21, 2018. This work was supported in part by the National Natural Science Foundation of China under Grant 61775050, in part by the Fundamental Research Funds for the Central Universities under Grant JD2017JGPY0005 and under Grant JZ2018HGTB0240. Corresponding authors: Zhongyi Guo and Kai Guo (e-mail: guozhongyi@hfut.edu.cn; kai.guo@hfut.edu.cn).

Abstract: Orbital angular momentum (OAM) in optical vortices (OV) beams offers a new dimension of space mode because coaxially propagating OV beams with different azimuthal OAM states are mutually orthogonal. As a result, the beams can be efficiently multiplexed and de-multiplexed to potentially increase the capacity of the optical communication system. Therefore, up to now, the azimuthal indices of the transverse spatial mode has been investigated for many times. This paper focuses on another mode, which can be called as radial indices of Laguerre–Gaussian beam. A novel OAM encoding system with high-order radial indices is established by simulation for the optical communication system. At the transmitter, a series of holograms of the Laguerre–Gaussian mode with different radial indices are used to achieve coaxial transmission of multiplexing beams, where each beam represents one data bit. At the receiver, we use the superposition of a conjugate light field corresponding to the transmitted beams for de-multiplexing the multiplexed beams. Meanwhile, the combination of the phase-shift factor and centroid algorithm can realize the simultaneous detection of the radial indices in each channel and efficient decoding of information. We also analyze the measurement deviation on the performance of an encoding system and give the corresponding discussions.

Index Terms: Free-space optical communication, optical vortices, multiplexing.

1. Introduction

With the development of electronic information technology, in order to eventually overcome unresolved bandwidth crunch problems, achieving higher data transmission capacity is one of the main directions of telecommunications. The ever-growing data-traffic has driven miscellaneous multiplexing approaches to enhancing transmission capacity and spectral efficiency. In the field of optical communications, a typical way to increase the transmission capacity is to multiplex multiple independent data channels. Common multiplexing methods focus on different time, wavelength, polarization, or spatial channel, corresponding to time-division multiplexing (TDM) [1], wavelength-division multiplexing (WDM) [2], polarization-division multiplexing (PDM) [3], and space-division multiplexing (SDM) [4], respectively. As a special case of SDM, mode-division multiplexing (MDM)

can be used, in which multiple orthogonal data carrying beams can be efficiently (de)multiplexed with little inherent crosstalk [5].

Orbital angular momentum (OAM), a nature of an optical vortices beam with a helical phase front, was revealed and demonstrated by Allen *et al.* in 1992 [6]. It was shown that the helical-phase beams comprising an azimuthal phase term of $\exp(il\varphi)$ have an OAM of $l\hbar$ per photon, where l (arbitrary integer) represents OAM states called topological charge, φ is azimuthal angle, and $\hbar$ is Plank's constant h divided by 2π [6]. In principle, vortex beams with different topological charges are mutually orthogonal and can be efficiently separated from each other even after spatially overlapping and coaxially propagating, which makes it possible to use the OAM states as a subset of MDM information channels to carry information in the field of free-space optical (FSO) communication and fiber optic communication system, including OAM shift keying (OAM-SK) system where each OAM state can represent a data bit, and OAM division multiplexing (OAM-DM) system where the vortex beams are treated as signal carriers [7]–[15]. Most of the OAM-based systems utilized the azimuthal index (l) of the vortex beam as a set of orthogonal bases that are treated as independent channels. In addition to the phase change in the azimuthal direction, beams carrying OAM may also have unique radial structures. One well-known OAM-carrying beam is the Laguerre-Gaussian (LG) beam. The LG beam is usually characterized by two indices: the azimuthal index (l) associated with OAM states which is mentioned above, and the radial index (p: a nonnegative integer) [15], which represents the number of rings for the vortex beam's intensity distribution in radial direction. Previous publications on OAM multiplexing focused on the orthogonality of LG beams with $p = 0$ but different l in a multiplexing system, while relatively little attention has been paid to investigating the p indices of LG beams. Recently, OAM-multiplexed FSO link using both the radial and azimuthal indices are explored [16]–[19], in which a FSO link by multiplexing four LG beams with $l = 0$ or 1 and $p = 0$ or 1 were demonstrated in [16], [17] and the power loss for nonzero p with limited receiver aperture were discussed in [18], [19]. In addition, it provides a useful basis for increasing the capacity of future optical communication systems [20]. All in all, most of the de-multiplexed method mentioned above is using phase pattern holograms and the order of used in the communication link is also relatively low. So, for the multiplexing link with different p indices, there are still some places that is worth to investigate, such as 1) establishment of more efficient multiplexing system with high order of p, 2) detection of p indices simultaneously and effectively, 3) impact of the crosstalk, 4) effect of the limited receiver aperture and so on.

In this paper, we focus on radial indices (p) of the OV beams and an OAM encoding system based on high order radial indices is established by simulation. At the transmitter, a series of holograms of Laguerre-Gaussian mode with same topological charge but different radial indices are used to achieve coaxial transmission of the multiplexing beams, where the information can be encoded. At the receiver, we use the conjugate light field corresponding to the transmitted beams to de-multiplex beams, and through the superposition of the phase-shift factor to redirect beams and using centroid algorithm to measure the according central intensities of bright spots accurately, the radial index of each channel can be detected simultaneously and the carried information can be decoded effectively. We have also analyzed the factors of measurement deviation of encoding system and tried to give the corresponding discussions.

2. Concept and Principle

2.1 The Laguerre-Gaussian Beams

In mathematical expression, the problem is cylindrically symmetric and can be expressed in cylindrical coordinates (r, φ, z), where r is the distance from the propagation axis, φ is the direction angle formed on the plane perpendicular to the propagation axis, and z is the distance along the propagation axis. One of these solutions of Helmholtz equation is the Laguerre-Gaussian (LG) function

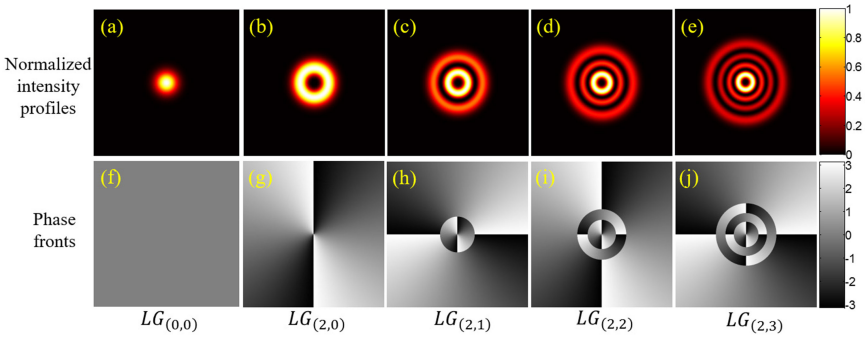

Fig. 1. Normalized intensity profiles and phase fronts of Laguerre-Gaussian ($L\,G_{(l,p)}$) beams with different azimuthal indices and radial indices. (a)–(e) intensity profiles of $L\,G_{(0,0)}$ (Gaussian-like beam), $L\,G_{(2,0)}$, $L\,G_{(2,1)}$, and $L\,G_{(2,3)}$. (f)–(j) phase fronts corresponding to (a)–(e).

and it can be expressed as [21], [22]:

$$u_{L\,G(l,p)}(r,\varphi,z) = \sqrt{\frac{2p!}{(\pi(p+|l|)!)}}\frac{1}{w(z)}\left(\frac{r\sqrt{2}}{w(z)}\right)^{|l|} L_p^{|l|}\left(\frac{2r^2}{w^2(z)}\right) \times \exp\left(\frac{-r^2}{w^2(z)}\right)\exp\left(\frac{-ikr^2z}{2R(z)}\right) \times \exp\left[i(2p+|l|+1)\tan^{-1}\frac{z}{z_R}\right]\exp(il\varphi), \quad (1)$$

where $k = 2\pi/\lambda$ is the wavenumber, λ is the wavelength, l and p are the topological charge and radial indices respectively, $w(z) = w_0\sqrt{1+(z/z_R)^2}$ is the Gaussian beam radius, w_0 is the beam waist, $z_R = \pi w_0^2/\lambda$ is the Rayleigh range, $L_p^{|l|}$ is the generalized Laguerre polynomial, and $(2p+|l|+1)\tan^{-1}(z/z_R)$ is the Gouy phase. It need be note that the phase profile, expressed as $exp\,(il\varphi)$, is what allows these beams to exhibit OAM [22]. An LG beam carrying OAM has two important characteristics: 1) a beam with $l \neq 0$ and $p = 0$ has a "doughnut" shape of intensity profile with a single-ring annulus and little power near the beam center; 2) a beam with $l \neq 0$ and $p > 0$ comprises $p+1$ concentric rings with a zero on-axis intensity. Normalized intensity profiles and phase fronts of Laguerre-Gaussian ($L\,G_{(l,p)}$) beams with different azimuthal indices and radial indices is shown in Fig. 1.

2.2 The Principle of Different Modes Detection

Importantly, two LG beams with the same beam waist are orthogonal to each other if they have either a different l values or a different p values. Based on this property, LG beams with different l or p can be multiplexed together, and l or p carried by one of the multiplexing beams can be detected precisely, indicating that multiple different LG beams could be employed for efficient channel multiplexing and de-multiplexing in optical communication links [16]. In most previous studies, the exploration of orthogonality has focused on different l, in this paper, we focus on radial indices p and the orthogonality of LG beams with same l but different p could be expressed as:

$$\left\langle u_{L\,G(l,p_m)}(r,\varphi,z)_m u^*{}_{L\,G(l,p_n)}(r,\varphi,z)_n \right\rangle \triangleq \int u_{L\,G(l,p_m)}(r,\varphi,z)_m u^*{}_{L\,G(l,p_n)}(r,\varphi,z)_n r dr d\varphi = \begin{cases} \int \left|u_{L\,G(l,p_n)}\right|^2 r dr d\varphi & m = n \\ 0 & \forall m \neq n \end{cases}, \quad (2)$$

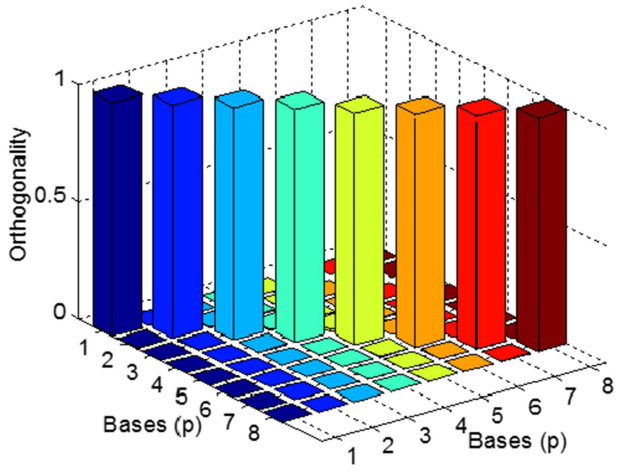

Fig. 2. Measured orthogonality relations between the bases formed by LG beams with different p values of 1–8.

where $*$ is the conjugate, and $\langle\rangle$ represents the inner product of two fields. In order to visually demonstrate this principle, we calculate the orthogonality relation between LG beams with different p values by taking the inner product of the two corresponding optical fields incorporating both amplitudes and phases, as shown in Fig. 2.

In our simulation, we simplified the above numerical calculation process and detected the mode by directly observing the product of the light field. The conjugate light field detection method is used to detect the p value, which is a method to determine the indices of a detected beam based on its orthogonality property. Given a transmitted LG beam, $u_{LG(l,p_m)}(r, \varphi, z)$, we calculate the product between the given LG beam and each of the mode set, $u^*_{LG(l,p_n)}(r, \varphi, z)$, where m and n represent the mth and nth beam. By using the orthogonality of the optical field, the beam that needs to be detected is multiplied with the conjugate light field, forming the product:

$$u_{\text{Detect}}(r, \varphi, z) = u_{LG(l,p_m)}(r, \varphi, z)_m u^*_{LG(l,p_n)}(r, \varphi, z)_n. \tag{3}$$

When the receiver receives the incoming optical vortex beam, we carry out the product of the vortex field with all the possible vortex beams, which can be expressed as:

$$u_{\text{Detect}}(r, \varphi, z) = u_{LG(l,p_m)}(r, \varphi, z)_m \sum_{n=1}^{N} u^*_{LG(l,p_n)}(r, \varphi, z)_n. \tag{4}$$

By using this conjugate light field detection method, we can realize the detection of p carried by one of the multiplexing LG beams. As shown in Fig. 3, for detecting the transmitted LG beam with $l = 1, p = 3$ as an example, we calculate its products with the support of mode set, conjugate light field of LG beams with same topological charge $l = 1$ but different radial indices $p = 1$, $p = 2$, $p = 3$, $p = 4$ and $p = 5$ respectively. By the product in (4), we detect intensity spot only at the center after the Fourier transform based on Lens imaging theory [23], if there is no doughnut or multi-ringed intensity profiles, then we can make sure the concrete mode. As shown in Fig. 3, the transmitted LG beam can be determined as the mode of $l = 1, p = 3$.

3. Multiplexing/De-Multiplexing System With Different Radial Indices

3.1 Multiplexing/De-Multiplexing System

Theoretically, LG beams with different azimuthal or radial indices are mutually orthogonal with each other, thus making it possible to utilize LG beams with higher order p for efficient multiplexing and de-multiplexing in a transmission system. Fig. 4 shows a simulated demonstration of a

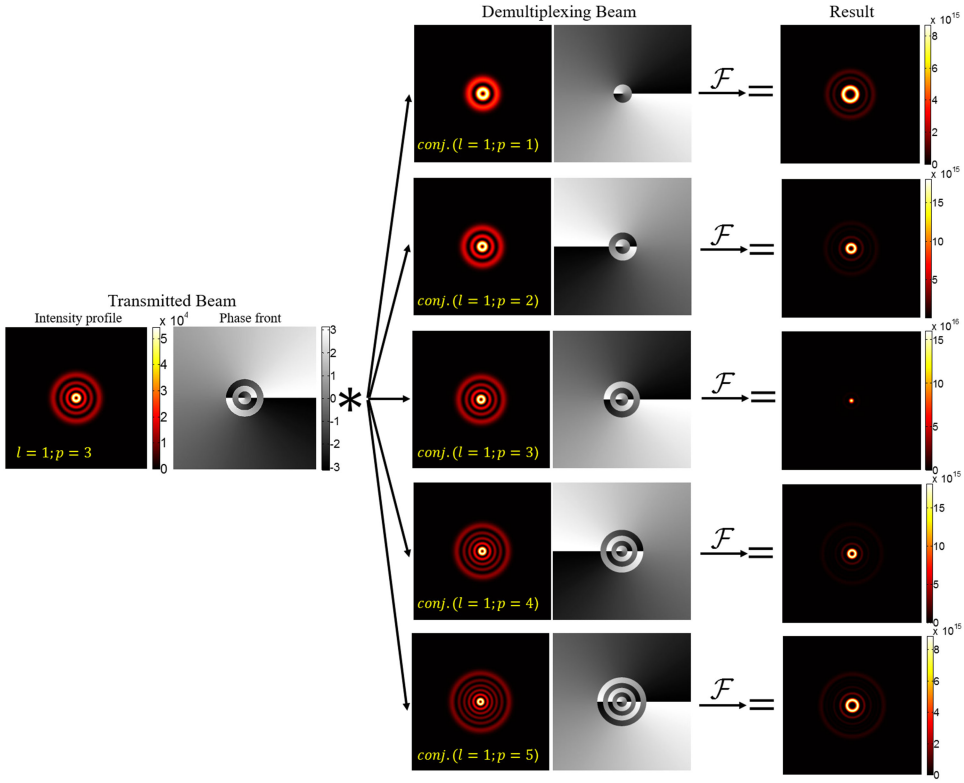

Fig. 3. The schematic of conjugate light field detection method to detect the radial indices of p value. The transmitted beam is $LG_{(1,3)}$, de-multiplexing beam are conjugate light field of $LG_{(1,1)}$, $LG_{(1,2)}$, $LG_{(1,3)}$, $LG_{(1,4)}$ and $LG_{(1,5)}$ respectively, the detected results are shown in the right column.

multiplexing/de-multiplexing system using multiple LG beams with same topological charge $l = 1$ but four different radial indices p {1, 2, 3, 4}. We firstly select a set of p values as the basis. At the transmitter, we simulate laser sources to produce Gaussian beams with wavelength (633 nm), beam waist (2 mm). Then, after dividing into four parts evenly, all splitting beams are radiating onto a series of holograms that are programmed with different modes for generating the Laguerre-Gaussian mode ($LG_{(l,p)}$) accordingly. By superposing four generated LG beams, we can achieve coaxial multiplexing transmission system of four LG modes including $LG_{(1,1)}$, $LG_{(1,2)}$, $LG_{(1,3)}$ and $LG_{(1,4)}$. And a piece of binary data signal, such as {1, 0, 1, 1}, can be encoded into the multiplexing vortex beam. At the receiver, the multiplexed beam is evenly divided into four parts by the splitter, and each part is multiplied by the conjugated basis corresponding to achieve de-multiplexing result. After being de-multiplexed, the vortex beam with target p values will be transformed to bright spots in the center position, and other beams still have bright rings accordingly. In order to detect the transformed central intensity distribution, a proper pinhole should be laid before the detector for choosing the central intensity. The measured result at the corresponding position is shown in right column of Fig. 4, from which we can measure the values of four light intensity distributions separately and plot them in a same chart after normalization of four data. Then, by setting the judgment threshold, the detector will transform the intensity distribution to the binary data signal of {1, 0, 1, 1}.

3.2 Method Optimization

As can be seen in Fig. 4, the receiver needs to split the received multiplexed beam into four parts before multiplying with the conjugate light field for detection, which is relatively complicated. So we have optimized the above method, through the superposition of holograms of conjugate light

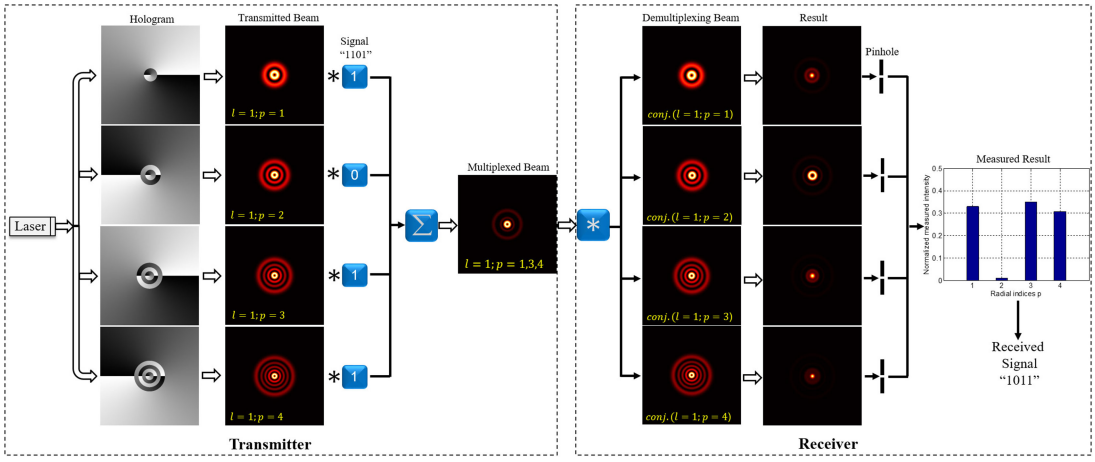

Fig. 4. Demonstration of a multiplexing/de-multiplexing system using multiple LG beams with four different radial indices.

field with additional phase-shift factor to achieve de-multiplexing and allow the redirection of the beams, the radial index of each channel can be detected in the same detection plane simultaneously, which reduces the complexity of the de-multiplexing system. The phase-shift factor can be expressed as $\exp[i2\pi(\mu x + \nu y)]$, where x is the horizontal coordinate, y is the vertical coordinate, $\mu = \sin\alpha/\lambda$, $\nu = \sin\beta/\lambda$, α and β are adjustable factors which represent the diffraction angles of horizontal and vertical directions. Due to the transforming property of Fourier transform, applying a phase-shift factor to the de-multiplexing plane at the receiver by controlling the μ and ν, we can easily manipulate the diffractive directions of de-multiplexed beams, thereby spatial displacement (μ, ν) can be achieved at the detection plane. After rewriting $\exp[i2\pi(\mu x + \nu y)]$ to Cylindrical coordinates as $exp\,(iK_n r)$ the de-multiplexing light field at the receiver can be described as:

$$u(r, \varphi, z) = \sum_{n=1}^{N} u^*_{LG(l,p_n)}(r, \varphi, z) exp\,(iK_n r). \tag{5}$$

As shown in Fig. 5(a), by using this method, the radial index of each channel can be detected in the same detection plane simultaneously, and Fig. 5(b) shows the measurement of four channels with high order p of $\{5, 6, 7, 8\}$ carrying binary data signal of $\{1, 1, 1, 1\}$. Moreover, this method can also be extended to detect more channels simultaneously, as shown in Fig. 5(c), giving an example of measuring eight channels carrying a piece of binary data signal of $\{1, 0, 1, 0, 1, 0, 1, 0\}$ in the same detective plane, which can reduce the complexity of the de-multiplexing system obviously.

Meanwhile, in order to measure multiple intensities of central bright spots in the same detection plane rapidly and accurately. We use the centroid algorithm to determine the position of the pinhole for detection. The particular algorithm steps can be described as follows: Firstly, divide the received intensity distribution image into N sub-images, each of which contains a single intensity that needs to be measured. Secondly, compute the sum of the gray scale of each pixel of sub-images and localize the centroid position. And the calculation method can be described as:

$$\begin{cases} x' = \dfrac{1}{I_0}\Delta x \Delta y \sum \left(I_{(x,y)} x\right) \\ y' = \dfrac{1}{I_0}\Delta x \Delta y \sum \left(I_{(x,y)} y\right) \end{cases}, \tag{6}$$

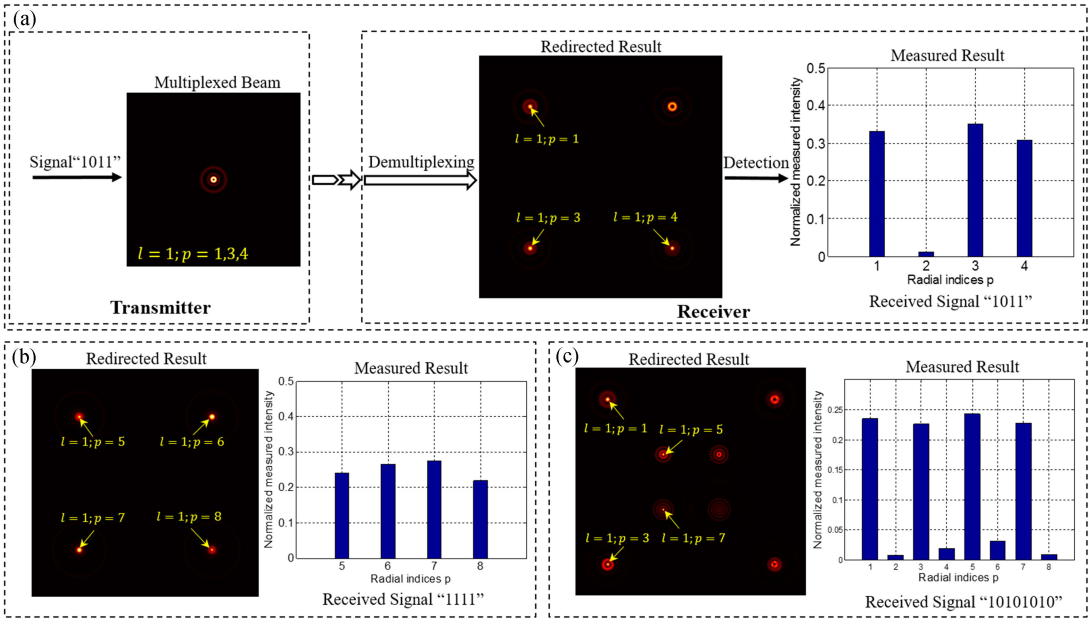

Fig. 5. Detection of the radial index of each channel simultaneously by additional phase-shift factor in simulation environment. (a) multiplexing and de-multiplexing of p {1, 2, 3, 4} carrying binary data signal of {1, 0, 1, 1}; (b) measuring four channels with high order p of {5, 6, 7, 8} carrying binary data signal of {1, 1, 1, 1}; (c) an example of measuring eight channels carrying a piece of binary data signal of {1, 0, 1, 0, 1, 0, 1, 0} in the same detection plane.

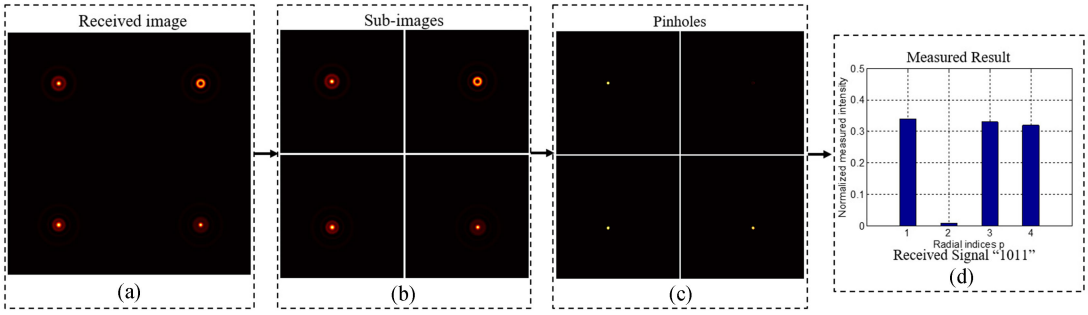

Fig. 6. The algorithm steps of measuring the weight of each single channel with different radial indices. (a) Received intensity distribution image at the receiver; (b) sub-images after being divided into four parts, each of which contains a single intensity that needs to be measured; (c) After pinholes locating the centroid positions respectively, the pinhole radius is 3 pixel in this figure; (d) measure the weight of each single channel with different radial indices.

where (x', y') represent the coordinate of the centroid position, $I_{(x,y)}$ is the intensity in the position (x, y), $\sum$ represents the sum of intensity in each sub-image and

$$I_0 = \Delta x \Delta y \sum I_{(x,y)}. \tag{7}$$

Then, set the detection pinhole in the position specified in preceding step, and do sampling by adopting an appropriate pinhole radius. Finally, measure the sum of the intensity scale of each pixel in the sampling area. After finishing all the sub-image calculations, the weight of each single channel with different radial indices can be obtained. The above processing steps are shown in Fig. 6.

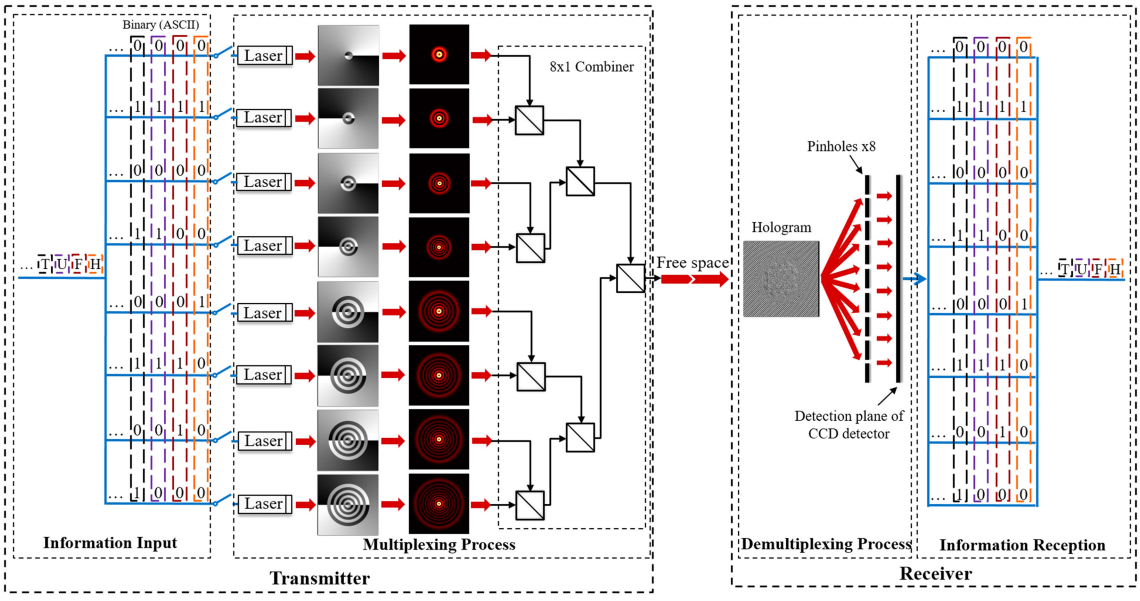

Fig. 7. The processes of an OAM encoding system with radial indices.

4. Demonstration of an OAM Encoding System With Radial Indices

By using the previously mentioned method, an OAM based data transmission system encoding with radial indices have been established by simulation. We select a set of radial indices p {1, 2, 3, 4, 5, 6, 7, 8} as the basis with same topological charge of $l = 1$, and use the coaxial-multiplexed LG beams to transmit the information "HFUTSCSIE" (The abbreviation of Hefei University of Technology, School of Computer Science and Information Engineering) by shift keying (SK). The process can be shown in Fig. 7.

At the transmitter, we convert each letter in "HFUTSCSIE" into binary data signal corresponding to the ASCII binary protocol. Then, the binary data signal streams corresponding to each letter are encoded to a multiplexing LG beams by switches which are used to control the "on" and "off" of each leaser link. Then different encoded beams are superposed by the 8x1 combiner system and transmit into free space. For example, the first letter "H" of "HFUTSCSIE" can be converted into eight bits binary data signals of {0, 1, 0, 0, 1, 0, 0, 0}. When the signal {0} comes, the switch will be turned off and corresponding single LG beam link block accordingly, in contrast, when the signal {1} comes, the switch will be turned on and corresponding single LG beam link can transmit. As a result, LG beam links with p values of {2, 5} can be transmitted and other LG beam links are blocked. In this way, eight bits digital information can be encoded to eight optional LG beams with different p values of {1, 2, 3, 4, 5, 6, 7, 8} respectively.

After transmitting through free space of 1 m, at the receiver, we use superposition of the conjugate light field corresponding to the transmitted beams to achieve beams' de-multiplexing, which can be achieved by setting a hologram with amplitude and phase. Meanwhile, the superposition of additional phase-shift factor are integrated into each conjugate light field to allow the redirection of beam and centroid algorithm are used in order to measure the multiple intensities of center bright spots accurately, therefore, the radial index of each channel can be detected on the detection plane of CCD detector simultaneously and effectively. In the process of signal decoding, we normalize the measured intensity and judge whether the received signal is {1} or {0} by setting the intensity judgment threshold. In our simulation, the judging threshold is set as 10% of total received power, and if the measured intensity value is higher than the judgment threshold we set, we can judge that the received signal is {1}, otherwise is {0} . After receiving eight binary signals, we convert them back to letters corresponding to the ASCII binary protocol and complete the decoding and recovering

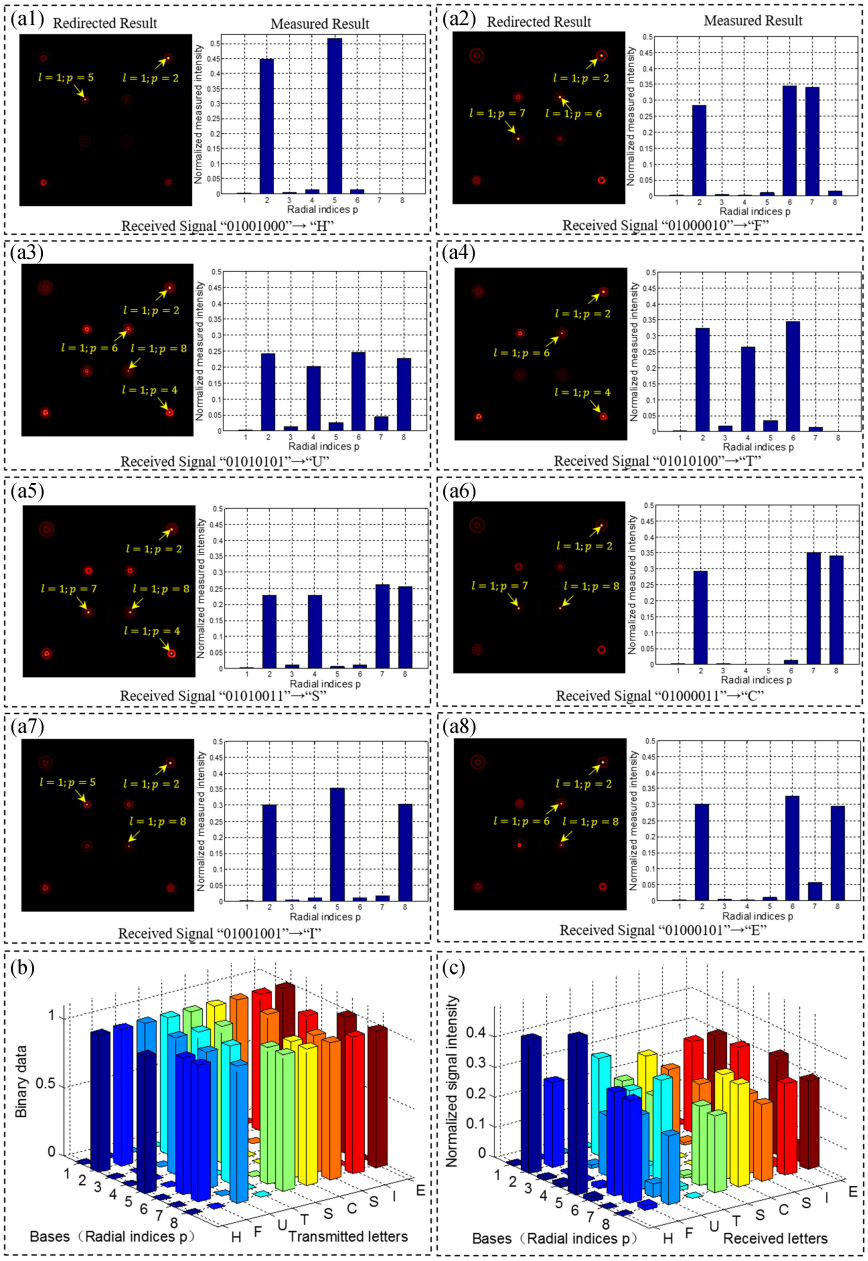

Fig. 8. The analysis results of an OAM encoding system with different radial indices. (a1)–(a8) the redirected result after de-multiplexing and the measured result of each latter; (b) the correspondence between transmitted letters and binary data, and mapping result to basis. (c) measured signal intensity obtained from the receiver.

information of "HFUTSCSIE". Fig. 8 shows the analysis results of an OAM encoding system with same topological charge but different radial indices. The redirected result after de-multiplexing and the measured result of each latter are shown in Fig. 8(a1)–(a8) respectively. Fig. 8(b) shows the correspondence between transmitted letters and binary data, which have been mapped to the basis of the chosen radial indices. The measured signal intensity obtained from the receiver is shown in Fig. 8(c) by normalizing the received signal intensity of each letter respectively (that is to say, the total intensity of the same color histogram in Fig. 8(c) is 1), matching well with the binary representations in Fig. 8(b).

It should be noted that the detectors can obtain the correct binary digital data by depending on whether there exist high bright spots at the center position, however, there are several factors affect the accuracy of the measurement results. When the interval between different p is small, crosstalk between adjacent modes will be relatively large, resulting from overlapping between bright spots and bright circles in the detection result. As shown in the most results of previous measurements, the intensity distribution is uneven. Therefore, we can enlarge interval between adjacent p values to reduce measurement deviation. On the other hand, the detection method mentioned in this paper relies on good alignment between the transmitter and the receiver. In fact, the misalignment between the transmitter and the receiver, including the lateral displacement and the angular deflection, also cause channel crosstalk [24]. In addition, the size of the receiving aperture has a great impact on the received optical signal power and detection accuracy of the system. Due to the effect of limited receiving aperture, the energy will not be concentrated completely at the correct position of the detection plane, therefore, at the receiver, the corresponding solution is to adjust the decision judgment appropriately so as to decide whether a mode is present or not in the signal. But it is worth noting that this method only applies to communication link based on OAM-SK. However, in OAM-DM-based communication links, this method is not applicable. Because the deviation in energy measurement will make the channel signal to noise ratio (SNR) very low and cause higher bit error rate (BER) correspondingly. Moreover, the introduced crosstalk will seriously affect the accuracy of the decoding result especially in long-distance transmission with turbulent environment, so considering that the turbulent environment brings about a large distortion of the phase, at the receiver before the decode processing, the recovery algorithm must also be set to reduce measurement deviation caused by turbulence, which can be further investigated for improving the performance of our encoding system in the future.

5. Conclusion

In summary, we have proposed and investigated a novel OAM encoding system based on the radial indices of p, in which the detection principle of different indices based on the orthogonality has been described in detail. Then, an OAM encoding system with different radial indices is established by simulation. At the transmitter, a series of holograms of Laguerre-Gaussian mode are used to achieve coaxial transmission of multiplexing beam with same topological charge but different radial indices, where the information can be encoded. At the receiver, we use the conjugate light field corresponding to the transmitted beams to de-multiplex beams. Through the superposition of the phase-shift factor and using centroid algorithm to redirect the de-multiplexed beams and measure the intensity distributions accordingly, the radial index of each channel can be detected simultaneously and the carried information can be decoding effectively. In the end, we analyze the measurement deviation on the performance of encoding system, and give the corresponding discussion.

References

[1] T. Richter *et al.*, "Transmission of single-channel 16-qam data signals at terabaud symbol rates," *J. Lightw. Technol.*, vol. 30, no. 4, pp. 504–511, Feb. 2012.
[2] A. Gnauck, P. Winzer, S. Chandrasekhar, X. Liu, B. Zhu, and D. Peckham, "Spectrally efficient long-haul WDM transmission using 224-Gb/s polarization-multiplexed 16-QAM," *J. Lightw. Technol.*, vol. 29, no. 4, pp. 373–377, Feb. 2011.
[3] X. Zhou *et al.*, "64-Tb/s, 8 B/s/hz, PDM-36qam transmission over 320 km using both pre-and post-transmission digital signal processing," *J. Lightw. Technol.*, vol. 29, no. 4, pp. 571–577, Feb. 2011.
[4] P. J. Winzer, "Making spatial multiplexing a reality," *Nature Photon.*, vol. 8, no. 5, pp. 345–348, 2014.
[5] S. Berdagué and P. Facq, "Mode division multiplexing in optical fibers," *Appl. Opt.*, vol. 21, no. 11, pp. 1950–1955, 1982.
[6] L. Allen, M. W. Beijersbergen, R. Spreeuw, and J. Woerdman, "Orbital angular momentum of light and the transformation of Laguerre-Gaussian laser modes," *Phys. Rev. A*, vol. 45, no. 11, pp. 8185–8189, 1992.
[7] G. Gibson *et al.*, "Free-space information transfer using light beams carrying orbital angular momentum," *Opt. Express*, vol. 12, no. 22, pp. 5448–5456, 2004.
[8] J. Wang *et al.*, "Terabit free-space data transmission employing orbital angular momentum multiplexing," *Nature Photon.*, vol. 6, no. 7, p. 488–496, 2012.

[9] J. Wang *et al*., "Experimental demonstration of 100-Gbit/s DQPSK data exchange between orbital-angular-momentum modes," in *Proc. Opt. Fiber Commun. Conf.*, 2012, Paper OW1I–5.
[10] H. Huang *et al*., "100 Tbit/s free-space data link enabled by three-dimensional multiplexing of orbital angular momentum, polarization, and wavelength," *Opt. Lett*., vol. 39, no. 2, pp. 197–200, 2014.
[11] M. Krenn *et al*., "Communication with spatially modulated light through turbulent air across vienna," *New J. Phys*., vol. 16, no. 11, 2014, Art. no. 113028.
[12] A. E. Willner *et al*., "Optical communications using orbital angular momentum beams," *Adv. Opt. Photon*., vol. 7, no. 1, pp. 66–106, 2015.
[13] C. Kai, P. Huang, F. Shen, H. Zhou, and Z. Guo, "Orbital angular momentum shift keying based optical communication system," *IEEE Photon. J*., vol. 9, no. 2, Apr. 2017, Art. no. 7902510.
[14] N. Bozinovic *et al*., "Terabit-scale orbital angular momentum mode division multiplexing in fibers," *Science*, vol. 340, no. 6140, pp. 1545–1548, 2013.
[15] M. Padgett and L. Allen, "The poynting vector in Laguerre-Gaussian laser modes," *Opt. Commun*., vol. 121, no. 1-3, pp. 36–40, 1995.
[16] G. Xie *et al*., "Experimental analysis of multiplexing/demultiplexing Laguerre Gaussian beams with different radial index," in *Proc. Frontiers Opt*, 2014, Paper FTh4B–6.
[17] G. Xie *et al*., "Experimental demonstration of a 200-Gbit/s free-space optical link by multiplexing Laguerre–Gaussian beams with different radial indices," *Opt. Lett*., vol. 41, no. 15, pp. 3447–3450, 2016.
[18] L. Lii *et al*., "Experimental demonstration of a 400-Gbit/s free space optical link using multiple orbital-angular-momentum beams with higher order radial indices," in *Proc. Conf. Lasers Electro-Opt*., 2015, pp. 1–2.
[19] L. Li *et al*., "Power loss mitigation of orbital-angular-momentum-multiplexed free-space optical links using nonzero radial index Laguerre–Gaussian beams," *JOSA B*, vol. 34, no. 1, pp. 1–6, 2017.
[20] A. Trichili *et al*., "Optical communication beyond orbital angular momentum," *Scientific Rep*., vol. 6, p. 27674, 2016, Art. no. 27674.
[21] H.-C. Kim and Y. H. Lee, "Hermite–gaussian and Laguerre–Gaussian beams beyond the paraxial approximation," *Opt. Commun*., vol. 169, no. 1–6, pp. 9–16, 1999.
[22] T. Doster and A. T. Watnik, "Laguerre–Gauss and Bessel–Gauss beams propagation through turbulence: Analysis of channel efficiency," *Appl. Opt*., vol. 55, no. 36, pp. 10 239–10 246, 2016.
[23] O. Bryngdahl, "Geometrical transformations in optics," *JOSA*, vol. 64, no. 8, pp. 1092–1099, 1974.
[24] Y. Zhao *et al*., "Feedback-enabled adaptive underwater twisted light transmission link utilizing the reflection at the air-water interface," *Opt. Express*, vol. 26, no. 13, pp. 16 102–16 112, 2018.